Solvation of fullerene and fulleride ion in liquid ammonia: Structure and dynamics of the solvation shells

ARTICLE *in* THE JOURNAL OF CHEMICAL PHYSICS · OCTOBER 2012

Impact Factor: 2.95 · DOI: 10.1063/1.4754852 · Source: PubMed

2 AUTHORS, INCLUDING:

Malay Kumar Rana
Indian Institute of Technology Kanpur
13 PUBLICATIONS **123** CITATIONS

SEE PROFILE

Solvation of fullerene and fulleride ion in liquid ammonia: Structure and dynamics of the solvation shells

Malay Kumar Rana and Amalendu Chandra

Citation: J. Chem. Phys. **137**, 134501 (2012); doi: 10.1063/1.4754852
View online: http://dx.doi.org/10.1063/1.4754852
View Table of Contents: http://jcp.aip.org/resource/1/JCPSA6/v137/i13
Published by the American Institute of Physics.

Solvation of fullerene and fulleride ion in liquid ammonia: Structure and dynamics of the solvation shells

Malay Kumar Rana[a] and Amalendu Chandra[b]
Department of Chemistry, Indian Institute of Technology, Kanpur 208016, India

(Received 8 July 2012; accepted 5 September 2012; published online 1 October 2012)

Molecular dynamics simulations have been performed to investigate the solvation characteristics of neutral fullerene (C_{60}) and charged fulleride anion (C_{60}^{5-}) in liquid ammonia. Potassium ions are present as counterions in the system containing fulleride ion. In addition to solvation characteristics, dynamical properties of solvation shells are also found out for both the neutral and anionic solutes. Our results reveal the presence of a rather large solvation shell of ammonia molecules around the C_{60}^{5-} ion. It is found that the ammonia molecules are more closely packed in the first solvation shell of C_{60}^{5-} than that of C_{60}. The distributions of ammonia molecules in the solvation shells of C_{60} and C_{60}^{5-} solutes together with hydrogen bonding characteristics of the solvent in different solvation shells are investigated. It is found that the solvation of the small counterions (K^+) in liquid ammonia is affected very little by the presence of the large C_{60}^{5-} anion. Regarding the dynamics of ammonia in solvation shells, it is found that the residence, translational and rotational dynamics of ammonia molecules differ significantly between the solvation shells of the neutral and charged fullerene solutes, especially in the first solvation shells. The average lifetimes of ammonia-ammonia hydrogen bonds are calculated from both continuous and intermittent hydrogen bond correlation functions. The calculations of binding energies reveal that the hydrogen bonds are weaker, hence short lived in the solvation shell of C_{60}^{5-} compared to those in the solvation shell of neutral C_{60} and also in bulk liquid ammonia.
 [http://dx.doi.org/10.1063/1.4754852]

I. INTRODUCTION

The solvation properties of fullerenes are of both practical and fundamental interest in many areas of science and technology. Specifically, the soluble form of C_{60} fullerenes has applications in biological sciences,[1–5] medicine,[6,7] biomedical imaging,[8,9] antioxidants,[10] bio-sensors,[11,12] and as chemotactic agents.[13] Those applications are generally conducted in aqueous environment of fullerene. The solvation of fullerenes in water has been investigated through many experiments to understand the microscopic details of such solvation and the so called hydrophobic interaction.[4,14–19] There have also been many theoretical studies of C_{60} solvation in water. Semi-empirical quantum mechanical calculations were conducted to investigate the effect of interaction of polar solvent on the structure and electronic properties of solvated fullerene.[19–23] It has been demonstrated that $C_{60}(H_2O)_{60}$ is the smallest energetically stable clathrate particle.[19] Keeping in mind for the advance applications of nanoparticle suspensions, it is necessary to understand the structural features and diffusion properties of nanoparticle suspensions. Direct experimental approaches are quite difficult to explore those properties. Molecular dynamics simulations, in this respect, plays valuable roles to provide insights into the microscopic properties in nanodimensions. Water mediated interaction between carbon nanoparticles and also carbon nanoparticle-water interactions have been investigated by employing this simulation method.[24–32] Atomistic molecular dynamics simulations of graphene plates, fullerenes, and carbon nanotubes in water[33–35] have revealed that the enthalpy factor rather than entropy prefers solvent separated fullerene or hydrophobic nanoparticles in water. Spatial and orientational aspects of water molecules adjacent to atomistic and coarse-grained C_{60} as well as inter-solute region between two C_{60} separated by a fixed distance have also been investigated. It was observed that the water molecules are densely packed and the dipole vectors stay tangential to the hydrophobic surface of C_{60}. A reduction of the number of hydrogen bonds from bulk value to ∼2.8 and ∼3.0 near the hydrophobic surfaces was observed for both the models.[36] So far, these studies show that hydrophobic hydration of nonpolar carbon nanoparticles gives rise to well-defined hydration shell of water around them. Large hydrophobic solutes break the hydrogen bonds between vicinal water molecules. Subsequently, dynamical properties such as translational-rotational mobilities, reorientational correlation and occupation time correlation function of water molecules in the solvation shell and inter-solute region of C_{60} were also calculated and, in general, a slower dynamics of water molecules in the vicinity of the solutes was reported.[37,38]

Fullerenes, because of their unique cage like structures with very high carbon density, are sparingly soluble in most common solvents.[39] Hence, it is important to find potent solvents where fullerenes would be more soluble so as to explore new fullerene reaction pathways for fullerene derivatives. Recently, fullerene-metal-ammonia solutions have been at the center of intensive research from experimental point of view to find out alternative routes for dissolution of neutral

[a]Present address: Department of Mechanical Engineering, University of Michigan, Ann Arbor, MI 48109-2133, USA.
[b]E-mail: amalen@iitk.ac.in.

fullerene without functionalization with hydrophilic groups. Apart from that, concentrated fulleride-metal-ammonia solutions are of practical interest, because of the presence of a variety of ionic and electronic species, such as solvated cation, solvated anion, and solvated electron. Thereby, it could serve as redox medium, charge storage, and medium for purification of fullerenes using solution techniques. Therefore, attention is also to be paid to the non-aqueous environments of fullerene C_{60} other than water. We choose liquid ammonia because it is an important solvent in many chemical reactions. Computer simulation studies of C_{60} or alkali metal fullerides in ammonia will reveal complexities associated with the solvation of neutral and charged carbon nanoparticles in a non-aqueous medium. Unlike water which forms on average about four hydrogen bonds in the liquid phase, ammonia in its liquid phase generally forms about two hydrogen bonds. This different hydrogen bonding capability may give rise to different characteristics of solvation of hydrophobic solutes like fullerenes in liquid ammonia compared to that in an aqueous medium. Experimentally, recent neutron diffraction findings have revealed the presence of giant solvation shells around C_{60}^{5-} in liquid ammonia.[40,41] A recent Monte Carlo study[42] looked at the energetics and local solvation structure of C_{60}^{n-} in liquid ammonia for $n = 0$, 2, 4 and 6. A progressively stronger hydrogen bonding of the ammonia molecules to the anion with increase of its negative charge was reported in this study. However, no noticeable orientational order was found for solvent molecules in the neighborhood of the neutral fullerene. In the present work, we have carried out molecular dynamics simulations to investigate the solvation behavior of neutral fullerene (C_{60}) and charged fulleride ion (C_{60}^{5-}) in liquid ammonia. We have employed the molecular dynamics simulation method in the present work so that, in addition to solvation energetics and structural aspects, dynamical properties of the solvation shell ammonia molecules can also be investigated for both neutral and anionic solutes. Specifically, we have looked at a number of issues related to solvation and dynamical properties like solvophobic interaction of C_{60} and solvophilic interaction of C_{60}^{5-} with polar ammonia molecules, microscopic structures of solvation shells, hydrogen bonding characteristics, translational and rotational motion of ammonia molecules and also hydrogen bond dynamics in solvation shells of C_{60} and C_{60}^{5-} solutes.

The organization of the rest of the article is as follows. In Sec. II, we describe our methodology and simulation details. We have discussed the solvation behavior of C_{60} and C_{60}^{5-} solutes in liquid ammonia in Sec. III. We have discussed solvent hydrogen bond and residence dynamics and also translational and rotational diffusion in different solvation shells around these solutes in Sec. IV. Finally, we have summarized our results and conclusions in Sec. V.

II. MODEL AND SIMULATION DETAILS

The molecular dynamics simulations have been carried out for (a) one neutral C_{60} solute dissolved in a solvent of 250 ammonia molecules and (b) five K^+ and one fulleride $C_{60}{}^{5-}$ ions dissolved in a solvent of 250 ammonia molecules. We refer to these two systems as System 1 and System 2, respectively. We note that the fullerene molecule (C_{60}) consists of 60 carbon atoms which are located at the vertices of each polygon with rigid bonds between the adjacent carbon atoms. It is the neutral hydrophobic solute under investigation in the present study. Each carbon atom carries zero charge in case of fullerene while the −5 charge is equally shared by the carbon atoms in the fulleride ion. The potassium ions in System 2 are modeled as charged Lennard-Jones particles.[43,44] The ammonia molecules are treated by four-site empirical simple point charge model, proposed by Gao *et al.*,[45] having rigid molecular framework. It is described by one nitrogen site with a partial charge of $q_N = -1.026$ and three hydrogen sites with a partial charge of $q_H = 0.342$.

The simulations of C_{60} or C_{60}^{5-} immersed in liquid ammonia are performed at 230 K. Non-bonded interactions between various species are represented by the following Lennard-Jones potential combined with Coulomb potential to account both van der Waals and electrostatic interactions

$$u(r_{ij}) = 4\epsilon_{ij}\left[\left(\frac{\sigma_{ij}}{r_{ij}}\right)^{12} - \left(\frac{\sigma_{ij}}{r_{ij}}\right)^{6}\right] + \frac{q_i q_j}{r_{ij}}, \quad (1)$$

where ϵ_{ij} is the Lennard-Jones well depth parameter and σ_{ij} is the Lennard-Jones diameter. Cross Lennard-Jones parameters are obtained according to Lorentz-Berthelot mixing rule. q_i and q_j are partial charges at two different atomic sites *i* and *j*. The non-bonded parameters for various species involved in simulation are given in Table I. The Lennard-Jones parameters for carbon atoms are taken from the original parametrization of Girifalco[46] reproducing the experimental crystal data of fullerenes. For each system, we started from equilibrated ammonia molecules at 230 K and at density 0.682 g cm^{-3} such that the simulated box had enough room to accommodate one fullerene. The box length was 22.908 Å for both the systems. For convenience, the neutral fullerene or the charged fulleride ion was placed at the center of the box and the entire system was further equilibrated for a period of 1 ns. Subsequently, the simulations were continued for another 2 ns for calculations of various structural and dynamical properties. The positions of all the carbon atoms were kept frozen during the simulation period. The Ewald sum method[47] were used to treat the long-range electrostatic interactions. We adopted the leap-frog algorithm for integration over time using a time step of 1 fs and the quaternion formulation was used for the rotational motion.[48] In addition to the two systems mentioned above, we also considered two larger systems of 763 ammonia molecules containing either a neutral fullerene molecule or a fulleride ion (C_{60}^{5-}) ion and five K^+ ions for looking at the possible system size effects on our calculated solvation

TABLE I. Charges and Lennard-Jones parameters for site-site interactions.

Atomic site	Charge (e)	σ (Å)	ϵ (kcal/mol)
N	− 1.026	3.36	0.210
H	0.342	0.0	0.0
C(C_{60})	0.0	3.47	0.066
C(C_{60}^{5-})	0.083	3.47	0.066
K^+	+1	3.331	0.100

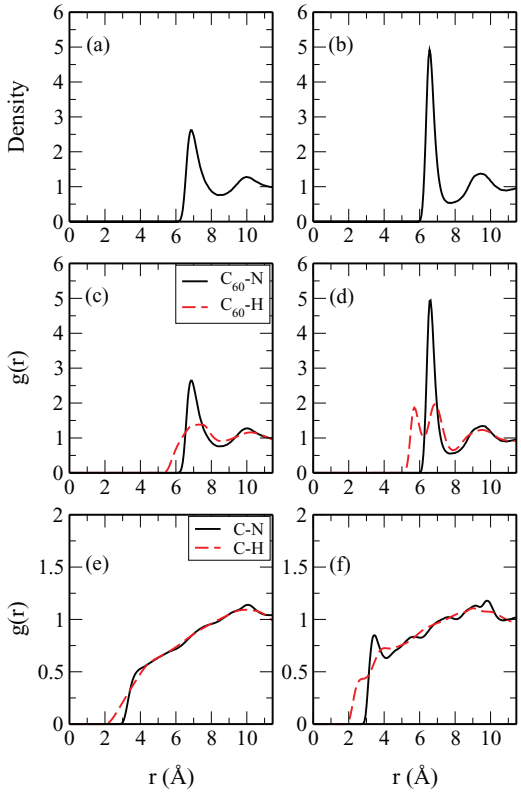

FIG. 1. The distributions of ammonia molecules around C_{60} (left panel) and C_{60}^{5-} (right panel) solutes. The results of (a) and (b) show the normalized number densities of NH_3 molecules around C_{60} and C_{60}^{5-} solutes. (c) and (d) The radial distributions of N and H atoms around the center of mass of C_{60} and C_{60}^{5-}. (e) and (f) C–N and C–H radial distribution functions.

properties. The simulations of these two larger systems were carried out in a cubic box of length equal to 32.66 Å. The two systems were equilibrated for 500 ps and then run for another 400 ps for calculations for various solvation properties which are discussed in Sec. III.

III. DISTRIBUTION OF AMMONIA MOLECULES

The density profiles of ammonia molecules around the center of mass of C_{60} and C_{60}^{5-} are shown in Fig. 1. A rather sharp and larger height of the first peak of the density profile associated with the C_{60}^{5-} compared to that of C_{60} means a profound solvation of the former with densely populated ammonia molecules in its first solvation shell. However, the width and height of the second peak corresponding to second solvation shell of C_{60}^{5-} do not differ in any significant manner from that of C_{60} implying that the charges of the fulleride ion do not have any substantial effects on the coordination structure beyond its first solvation shell. The first and second solvation shells of C_{60} and C_{60}^{5-} spreading over 6.07 − 8.56 Å, 8.56 − 11.45 Å and 5.92 − 7.82 Å, 7.82 − 10.92 Å contain 44, 82 and 41, 78 ammonia molecules, respectively. The corresponding experimental values for the coordination numbers of the fulleride ion in its first and second solvation shells are 44.6 and 79.6, respectively.[41] Also, the first solvation shell of the fulleride ion extends up to 7.8 Å in our calculations which can be compared with the corresponding experimental value

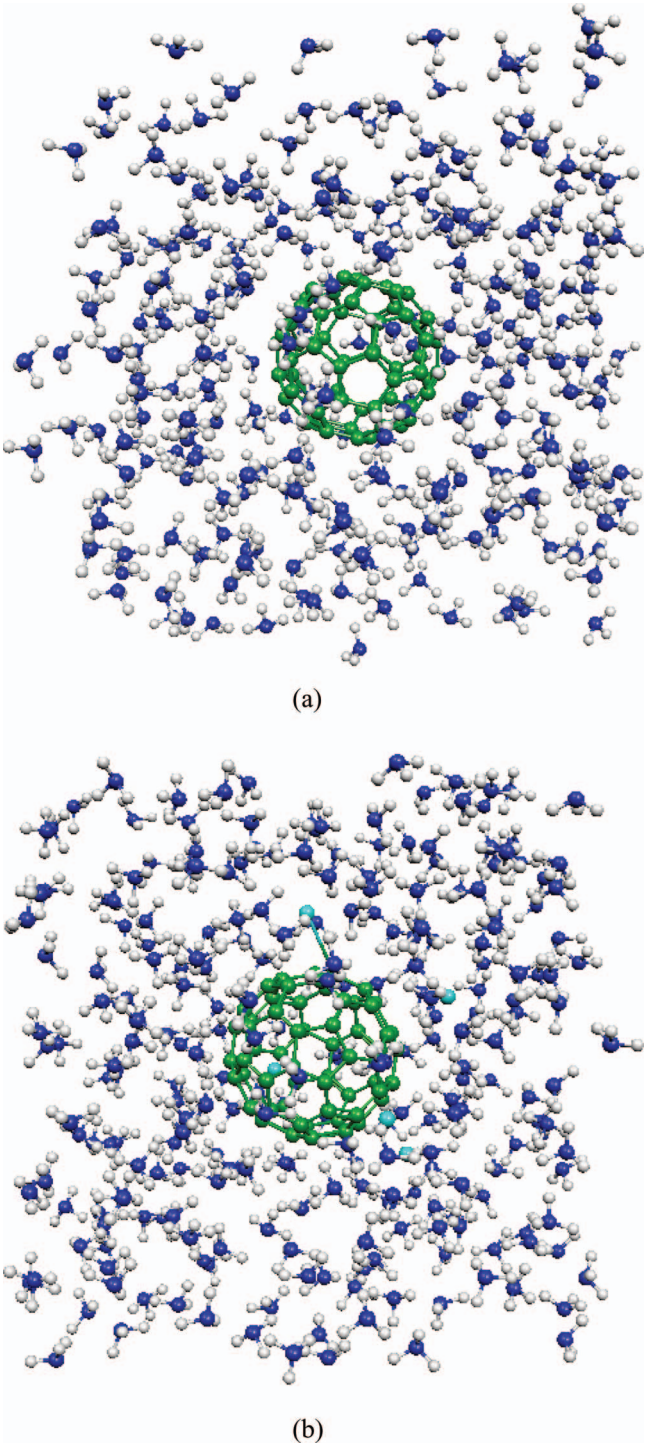

FIG. 2. Snapshots of configurations of ammonia molecules around (a) C_{60} (top) and (b) C_{60}^{5-} (bottom).

of 7.5 Å.[40,41] A shift of the first solvation shell by 0.15 Å toward the surface of fullerene is found in our study as we move from C_{60} to C_{60}^{5-}. This can be attributed to an enhanced attraction between anionic fullerene with ammonia molecules that gives rise to closer approach of ammonia molecules as well as a tighter packing of them around the anion (see also the snapshot given in Fig. 2 where ammonia molecules are seen to approach closer to the anionic fullerene). This is also seen from the narrow span of the first solvation shell of C_{60}^{5-}

over approximately the same number of solvent molecules compared to that of C_{60}. It would also be instructive to find out the average number density of ammonia molecules in the solvation shells of the neutral and charged solutes and compare these average densities with those of the bulk. The average number densities of the first solvation shells are calculated by integrating the position dependent density profiles of Figs. 1(a) and 1(b) over the regions of the first solvation shells as mentioned above. Such calculations reveal that the average number densities of the first solvation shells of the neutral and charged solutes are, respectively, 1.2 and 1.6 times the average bulk density. Thus, it is seen that the average number density of ammonia molecules in the first solvation shell of the fulleride ion is significantly higher than the corresponding density of the first solvation shell of the neutral fullerene. Clearly, the dipolar ammonia molecules do not solvate a neutral solute as strongly as it does for a charged solute. This is a manifestation of the solvophobic effect which arises from the details of solute-solvent interactions and the modifications of solvent-solvent interactions due to the presence of the solute. The presence of the negative charge on C_{60}^{5-} plays the key role for stronger solvation and bringing the solvent molecules closer to the anionic fullerene which is further ascertained from the radial distribution plots of $g_{CH}(r)$ and $g_{CN}(r)$ given in Fig. 1. The first peaks of $g_{CN}(r)$ and $g_{CH}(r)$ for C_{60}^{5-} are found to be located at 3.4 and 2.65 Å, respectively, which can be compared with the corresponding experimental values of 3.3 and 2.6 Å for the same anionic solute.[41] The coordination numbers as obtained by integrating the first peak region of $g_{CN}(r)$ and $g_{CH}(r)$ for the anionic solute are found to be 3.0 and 2.0 Å, respectively. The corresponding experimental coordination numbers are, respectively, 3.2 and 2.3 Å.[41] The radial distribution functions (RDFs) for C_{60}^{5-} appear more toward the solute than that for the neutral fullerene. The appearance of strong peaks in $g_{CH}(r)$ and $g_{CN}(r)$ for C_{60}^{5-} is attributed to the well-defined solvation structure around C_{60}^{5-} while they get broadened in case of C_{60} due to solvophobic effect arising from the interaction between non-polar C_{60} and polar ammonia molecules. The average nearest neighbor C···H distance is found to be 2.65 Å for the fulleride ion which bears the signature of weak (C_{60}^{5-})···H–N hydrogen bonds. The presence of such weak hydrogen bonds is also responsible for the difference in structure of the C_{60}–H and C_{60}^{5-}–H distribution functions as seen in Figs. 1(c) and 1(d). We note that such weak hydrogen bonds have also been observed in solid phase of $(ND_3)_xNaA_2C_{60}$ class of compounds ($0.7 \leq x \leq 1$, A = K, Rb).[49] Thus, one of the hydrogen atoms of NH_3 molecules points toward the surface of C_{60}^{5-} (as revealed from $g_{C_{60}-H}(r)$ of Fig. 1(d) as well, where the first peak for C_{60}–H RDF appears before the RDF of C_{60}–N). For the neutral fullerene system, such behavior is not observed so prominently as seen in $g_{C_{60}-H}(r)$ of Fig. 1(c) and $g_{CH}(r)$ of Fig. 1(e). In fact, calculations of the orientational distributions of the angle between the N–C_{60} and N–H vectors reveal a most probable angle of ∼80° for the neutral solute and ∼20° for the charged solute. In these calculations, the ammonia molecules residing up to the first maximum of the C_{60}–N correlations were considered for both the neutral and the charged solutes. Thus, the N–H bonds prefer a parallel orientation with respect to the surface for the neutral C_{60} solute. We note that a similar parallel orientation was also found for water molecules near a neutral surface.[50] In case of the charged solute, the N–H bonds prefer a different orientation that favors formation of weak hydrogen bonds with the negatively charged carbon atoms of the solute. The fulleride ion remains surrounded with five K^+ ions at an average distance ∼6.01 Å (Fig. 3(a)). The five K^+ ions belong to a shell extending from 5.7 to 7.0 Å. We note in this context that the C_{60}^{5-} ion is solvated by both K^+ ions and NH_3 molecules. While there are five K^+ ions in the neighborhood of the fulleride ion, the total coordination number of the anion is about 46 which means, in addition to the K^+ ions, about 41 NH_3 molecules are also found to reside in the first solvation shell of the fulleride ion. This picture is also supported by the substantial overlap of the fulleride-K^+ and fulleride-N radial distributions functions along the distance axis in the region of the first solvation shell of the C_{60}^{5-} ion. As common phenomenon like metals undergoing extensive solvation in liquid ammonia, here K^+ ions are also strongly solvated by ammonia molecules as evident from $g_{KN}(r)$ and $g_{KH}(r)$ plots in Fig. 3(b). The coordination number calculated from the first solvation shell (2.54–3.82 Å) of K^+−N radial distribution function is 5.5 for K^+ which is in good agreement with previous results.[51] The average K–N distance for solvation shell ammonia molecules is found to be 2.90 Å which is close to that in potassium-ammonia solution (∼2.88, 2.85 Å) reported earlier.[51,52] Thus, the C_{60}^{5-} ion does not play a major role in K^+ ion solvation. In both the neutral and ionic solutions, the features such as average N···N, H···H, N···H distances corresponding to principal peaks occurring at 3.3, 2.8, and 2.4 Å (Fig. 4) corroborate with the experimental findings.[53,54] The peak at 3.6 Å of $g_{NH}(r)$ is assigned for non-hydrogen bonded van der Waals contacts between ammonia molecules.

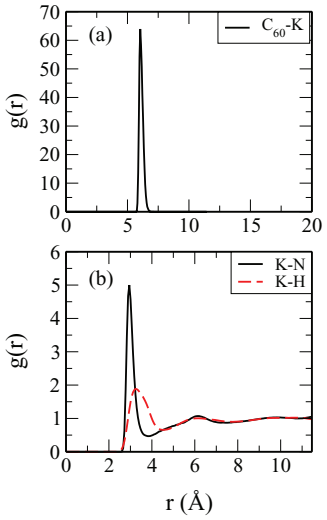

FIG. 3. (a) The distribution of K^+ around the center of mass of C_{60}^{5-}, (b) K–N and K–H radial distribution functions.

The number of N···H−N hydrogen bonds formed per ammonia molecule in solvation shells of C_{60} and C_{60}^{5-} are shown in Fig. 5. The two neighboring NH_3 molecules are taken to form a hydrogen bond if the N···N and N···H distances are

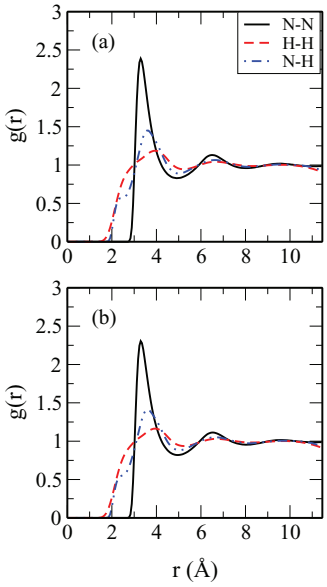

FIG. 4. The site-site radial distribution functions of NH_3 molecules in (a) System 1 and (b) System 2.

less than or equal to 5.0 and 2.63 Å, respectively, which are the distances of first minima of the corresponding radial distribution functions. In both cases, ammonia molecules loose significant number of hydrogen bonds near the surface of fullerenes. For the solution with the fulleride ion, some of the ammonia molecules are also involved in solvating potassium ions and this solvation process reduces the average number of hydrogen bonds per ammonia molecule in solvation shells away from the C_{60}^{5-} compared to the corresponding hydrogen bonding results for solution with the neutral solute. The average number of H-bonds per ammonia molecule (n_{HB}) decreases from 2.8 for bulk ammonia to ∼2.2 and 2.15 near the C_{60} and C_{60}^{5-} solutes. In the second solvation shells, the corresponding hydrogen bond numbers are found to be 2.6 and 2.4 for C_{60} and C_{60}^{5-}, respectively, which are closer to the corresponding bulk value. We note that no angle cutoff has been used in the hydrogen bond definition in the present study. Inclusion of such an angle cutoff would reduce the number of hydrogen bonds both in the solvation shells of the solutes and also in bulk ammonia.[55]

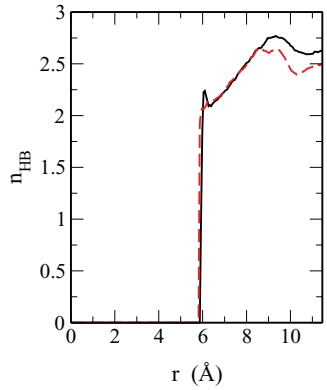

FIG. 5. The hydrogen bond profiles for the NH_3 molecules surrounding C_{60} (solid line) and C_{60}^{5-} (dashed line).

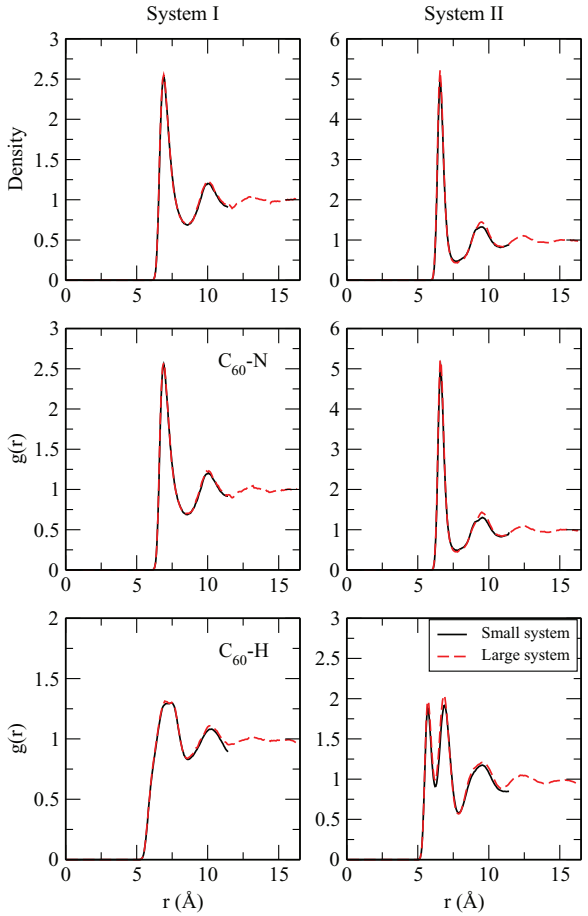

FIG. 6. The distributions of ammonia molecules around C_{60} (left panel) and C_{60}^{5-} (right panel) solutes for smaller (solid) and larger systems (dashed curves). Note that the smaller and larger systems differ in the number of ammonia molecules which is 255 for the smaller system and 763 for the larger system.

Finally, before we close our discussions on the structural aspects of fullerene and fulleride ion solvation in liquid ammonia, we would also like to comment on the possible effects of system size on the results presented above. For this purpose, we have compared ammonia density profiles around the solutes and some of the RDFs presented above with those of a much larger system consisting of 763 water molecules and the solute(s) in Fig. 6. As can be seen from this figure, no significant differences in the density profiles and RDFs could be found between the results of the smaller and the larger systems except that the larger system allows us to calculate the density profiles and RDFs over larger distances. The coordination numbers of the first (second) solvation shells for the fullerene and fulleride solutes for the larger systems are found to be 44 (85) and 40 (77) which can be compared with the corresponding values of 44 (82) and 41 (78), respectively, for the smaller systems. In view of the above results, we present the dynamical results for the smaller systems only in Sec. IV.

IV. DYNAMICS OF AMMONIA MOLECULES

A. Survival probability functions and residence times

We have calculated both intermittent and continuous survival probability distribution functions[56] for ammonia

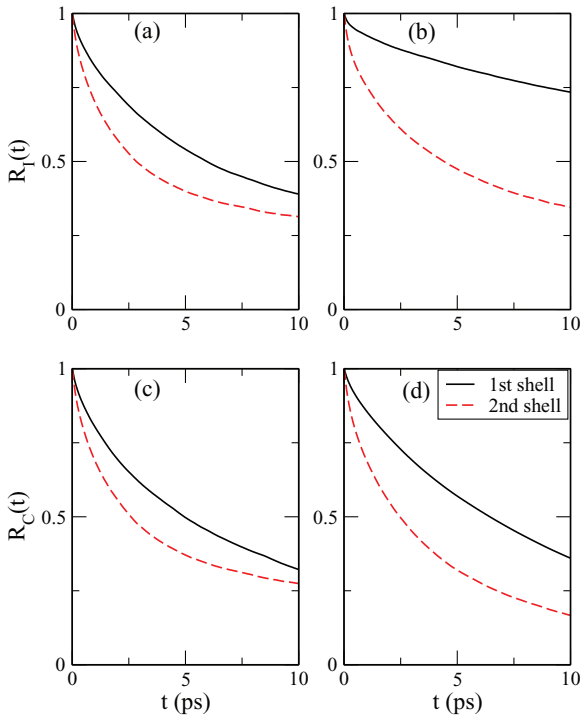

FIG. 7. The decay of the residence probability functions of ammonia molecules in solvation shells of the neutral and charged solutes. The left panel is for System 1 (C_{60} in ammonia) and right panel is for System 2 (C_{60}^{5-} in ammonia). The plots of (a) and (b) show the decay of intermittent residence probability functions, $R_I(t)$ and those of (c) and (d) show the decay of continuous residence probability functions, $R_C(t)$ for the two systems. The solid line is for the first solvation shell and the dashed line is for the second solvation shell.

molecules in the solvation shells of neutral and charged fullerene. The intermittent survival probability function $R_I(t)$ is defined as

$$R_I(t) = \langle \phi_i(0)\phi_i(t)\rangle / \langle \phi_i(0)^2\rangle. \quad (2)$$

$\phi_i(t) = 1$ if ith molecule is found in a given region at time t provided that it was also in the same region at time 0, else $\phi_i(t) = 0$. The time dependent continuous survival probability function $R_c(t)$ is defined as

$$R_C(t) = \langle \phi_i(0)\Phi_i(t)\rangle / \langle \phi_i(0)^2\rangle, \quad (3)$$

where $\Phi_i(t) = 1$ if ith solvent molecule is continuously found in a given region from time 0 up to time t without ever getting out of the region in the interim period, otherwise it is zero. The time dependence of the probability functions is shown in Fig. 7. The probability functions show initially faster relaxation followed by slower relaxation. The average residence times are calculated by integrating the above correlation functions. We denote τ_I as the intermittent residence time and τ_C as the continuous residence time. The relaxation of the probability functions is found to occur at a slower rate in the first solvation shells compared to that in the second solvation shells for both the solutes which can be attributed to solute-solvent correlations present in the systems. Between the first solvation shells of the neutral and the charged solutes, the decay is found to be slower for the charged solute compared to that for the neutral one due to stronger interactions of the solvation shell ammonia molecules with the negative charges of the fulleride ion. The integrated residence times (both intermittent and continuous) of ammonia molecules are presented in Table II. For both the solutes, the values of τ_I and τ_C are higher for the first solvation shells than second solvation shells which implies that the solvent molecules in the second shells move more freely due to reduced effects of the solutes. As discussed above, the values of $\tau_{I,C}$ in the first solvation shell of the fulleride ion are higher than that of the neutral fullerene. This is due to more frequent exchange of the ammonia molecules between the first and second solvation shells in the latter case where the attractive interaction between the solute and solvent molecules is relatively less. In particular, we see a significant slowing down of the decay of the first solvation shell intermittent correlation than that of the continuous one as we move to the charged C_{60}^{5-} solute from the neutral C_{60}. Since the intermittent correlation allows recrossing of the dividing surface between the first and the second solvation shells, its dynamics captures the slower local structural relaxation of ammonia molecules around the solutes. Such slower local structural relaxation is governed primarily by the long-time diffusion which is considerably slowed down for ammonia molecules in the solvation shells of the fulleride ion due to electrostatic interactions with the charged solute (see Sec. IV B). Hence, the intermittent residence time of ammonia molecules in the first solvation shell of C_{60}^{5-} is found to be significantly longer than that for the neutral C_{60} solute. The values of $\tau_{I,C}$ for second solvation shells of the solutes show, however, a reverse trend, i.e., the second solvation shell of C_{60} has a higher residence time than that for C_{60}^{5-}. This is likely due to the relatively bigger second solvation shell of C_{60} compared to that of C_{60}^{5-}.

TABLE II. The continuous and intermittent residence times of ammonia molecules obtained from the integrals of the respective survival probability functions and diffusion coefficients as calculated from VCF.

Shell	τ_I (ps)	τ_C (ps)	D (10^{-5} cm^2 s^{-1})
		System 1	
1	11.24	8.8	5.67
2	10.20	8.24	6.96
		System 2	
1	38.25	9.85	2.14
2	9.60	5.0	5.75
Bulk			6.73

B. Translational dynamics

We have calculated the relaxation of solvent velocity autocorrelation functions (VCFs) to measure the solvent translational motion in different regions around the neutral and charged solutes. The diffusion coefficient (D) values are extracted by integrating the velocity autocorrelation functions ($C_v(t)$) as follows:

$$C_v(t) = \frac{\langle v_i(0)v_i(t)\rangle}{\langle v_i(0)^2\rangle}, \quad (4)$$

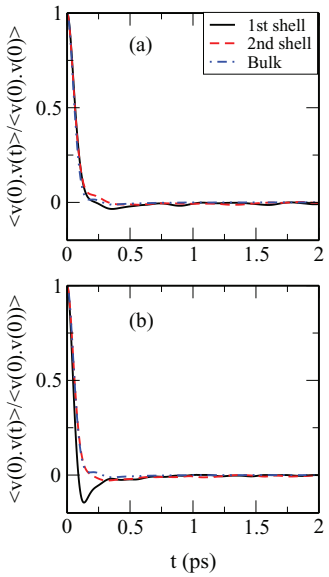

FIG. 8. The plots of velocity autocorrelation functions in different solvation shells for (a) System 1 and (b) System 2.

$$D = \frac{k_B T}{m} \int_0^\infty C_v(t)\, dt, \tag{5}$$

k_B is the Boltzmann constant, T is absolute temperature, and m is the mass of an ammonia molecule and the average of Eq. (4) is over all the ammonia molecules that were found to be in a given solvation region at time $t = 0$. We note that since the residence time of ammonia molecules in a given solvation shell is much longer than the time scale of velocity relaxation, an ammonia molecule which was in a given solvation shell at the initial time is expected to remain mostly in the same solvation shell over the period of its velocity relaxation. The plot of VCF of solvent molecules for systems containing the neutral and ionic solutes are shown in Fig. 8. The greater negative dip of VCF in the first solvation shell of C_{60}^{5-} compared to others is the result of stronger correlation and more pronounced caging effect produced by stronger ion-dipole interaction between C_{60}^{5-} and ammonia molecules. Thus, the ammonia molecules in the first solvation shell of C_{60}^{5-} undergo slower diffusion (Table II). The presence of this interaction lowers the diffusion coefficient values in both the first and second solvation shells of C_{60}^{5-} than that of C_{60} whose interaction with the solvent molecules is solvophobic in nature. Both kinds of interactions are dominated more in the first solvation shells of the solutes rather than the distant ones, hence, the solvent molecules in the second shell are more mobile than that in the first solvation shell. It is also seen that the difference in solvent diffusion coefficient values between the second solvation shells of C_{60} and C_{60}^{5-} is relatively smaller than that of their first solvation shells.

C. Orientational dynamics

The orientational dynamics of ammonia molecules around the neutral and charged solutes are investigated by calculating the time dependence of dipole orientational time correlation function $C_\mu^{(l)}(t)$ which is defined as

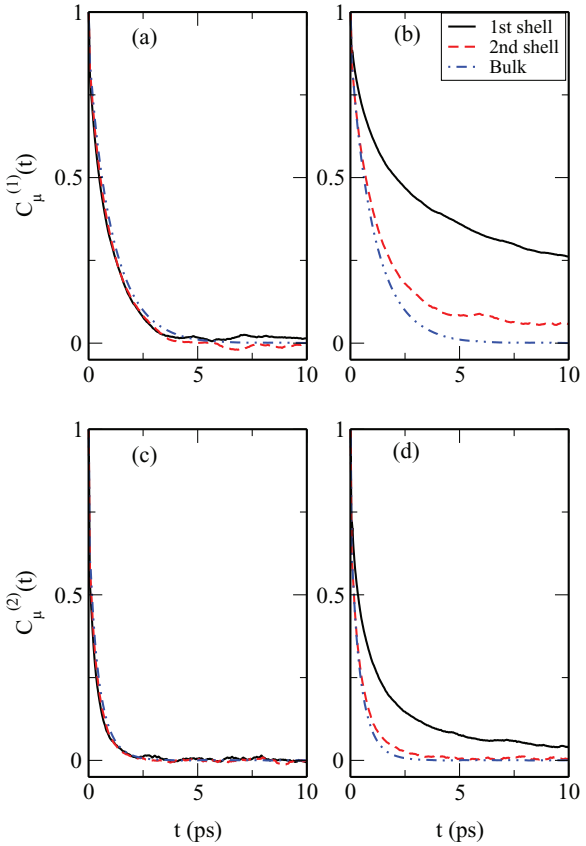

FIG. 9. The relaxation of the dipole vectors of solvent molecules around C_{60} and C_{60}^{5-}. (a) and (b) Decay of the first rank and (c) and (d) show the decay of the second rank dipole correlation functions. The left and right panels are for C_{60} and C_{60}^{5-} solutes, respectively.

$$C_\mu^{(l)}(t) = \frac{\langle P_l(\mu(t) \cdot \mu(0))\rangle}{\langle P_l(\mu(0) \cdot \mu(0))\rangle}, \tag{6}$$

where P_l is the Legendre polynomial of order l and $\mu(t)$ is the unit vector along the dipole moment vector of a solvent molecule at time t. The solvent molecules present in a given solvation shell at time $t = 0$ only contribute to $C_\mu^{(l)}(t)$ of that solvation shell. The time dependence of first ($l = 1$) and second ($l = 2$) order dipole correlation functions of ammonia molecules in solvation shells of C_{60} and C_{60}^{5-} around the solutes as well as in the bulk region are shown in Fig. 9. The correlation functions reveal two time constants corresponding to the short and long time parts of their decay. The average orientational relaxation times calculated from the integrals of the corresponding correlation functions are presented in Table III. Ammonia molecules around neutral C_{60} in both solvation shells have very similar decay trends of their dipole vectors and hence have very close relaxation times. On the other hand, strong electrostatic interaction between C_{60}^{5-} and proximal ammonia molecules leads to a slower decay of the dipole correlation functions. Here, the values of τ_μ^l (l = 1, 2) in the first solvation shell of C_{60}^{5-} are significantly higher than that of the second solvation shell. This shows substantial amount of solvophilic interaction between the charged solute and the solvent. We have also calculated the rotational

TABLE III. First and second order time constants (in ps) for the relaxation of dipole vector, N−H and H−H bond vectors of ammonia molecules. The time constants are expressed in ps.

Shell	τ_μ^1	τ_μ^2	τ_{NH}^1	τ_{NH}^2	τ_{HH}^1	τ_{HH}^2
			System 1			
1	0.87	0.28	0.52	0.23	0.48	0.22
2	0.89	0.30	0.63	0.26	0.59	0.25
			System 2			
1	6.96	1.36	1.63	0.59	1.01	0.65
2	1.91	0.40	0.85	0.31	0.67	0.30
Bulk	1.00	0.34	0.68	0.29	0.63	0.28

relaxation of N–H and H–H vectors by means of the following orientational correlation functions:

$$C_\alpha^{(l)}(t) = \frac{\langle P_l(\alpha(t)\cdot\alpha(0))\rangle}{\langle P_l(\alpha(0)\cdot\alpha(0))\rangle}, \quad (7)$$

where α is the unit vector pointing toward the N–H or H–H vectors. The decay profiles of the N–H bond vectors (shown in Fig. 10) show bimodal behavior and follow similar trends as found for the relaxation of molecular dipole vectors discussed before and also of H–H vectors (results not shown). The integrated relaxation times for N–H and H–H bond vectors given in the same Table III. These results again ascertain that the stronger solute-solvent correlation and close proximity hinder rotation of molecular vectors for solvation shell ammonia molecules around the charged fulleride solute.

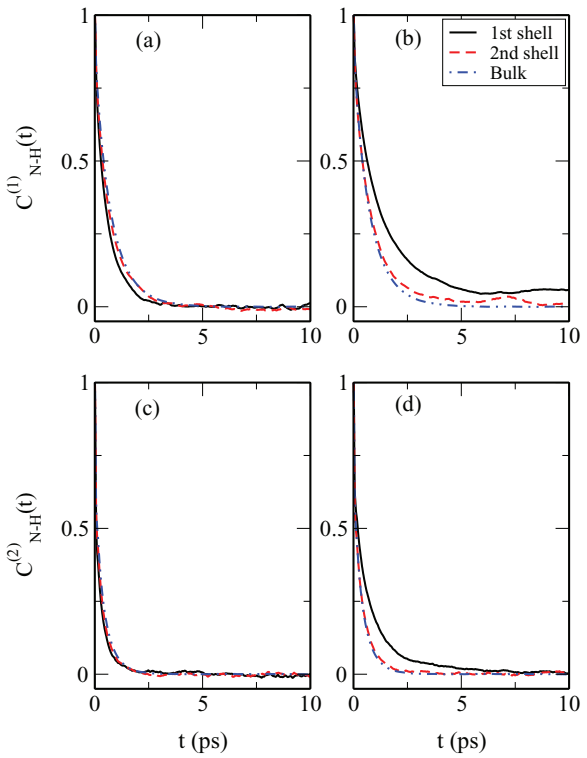

FIG. 10. The relaxation of N–H bond vectors of solvent molecules around C_{60} and C_{60}^{5-}. (a) and (b) First rank and (c) and (d) are for second rank correlations. The left and right panels are as in Fig. 9.

D. Hydrogen bond dynamics

We have looked into the dynamics of N−H···N H-bonds of ammonia molecules surrounding C_{60} and C_{60}^{5-} solutes and how these dynamics are different from the corresponding bulk properties. We have calculated the continuous hydrogen bond time correlation function defined as[56–61] $S_{HB}(t) = \langle h(0)H(t)/h(0)^2\rangle$ where the hydrogen bond variable $h(t) = 1$ if a tagged pair of ammonia molecules are hydrogen bonded at time t, otherwise, it is zero. The dynamical variable $H(t) = 1$, if the tagged pair of ammonia molecules remain continuously hydrogen bonded since time 0 to t, else it is zero. The time integral of the correlation function $S_{HB}(t)$ gives the average H-bond lifetime τ_{HB}. The probability that the two ammonia molecules remain hydrogen bonded at time t given that they were hydrogen bonded at time 0, is given by intermittent hydrogen bond correlation function $C_{HB}(t)$ which is defined as[56–64] $C_{HB}(t) = \langle h(0)h(t)/h(0)^2\rangle$. Thus, $C_{HB}(t)$ allows breaking and reformation of hydrogen bonds in the interim period and provide information about structural relaxation of hydrogen bonds. In addition, we define another correlation function $N_{HB}(t)$ which is the probability of two ammonia molecules remaining as nearest neighbors without being hydrogen bonded given that they were hydrogen bonded at time $t = 0$.[56,63,64] The two correlation functions, $C_{HB}(t)$ and $N_{HB}(t)$ can be put together to describe the kinetics of hydrogen bond breaking and reformation events with a simple rate equation[59,62]

$$-\frac{dC_{HB}(t)}{dt} = k_{HB}C_{HB}(t)(t) - k'_{HB}N_{HB}(t), \quad (8)$$

where k_{HB} and k'_{HB} are forward and backward rate constants. The average lifetime of N−H···N hydrogen bonds is extracted from the inverse of k_{HB} using the above equation and the simulated data.

The time dependence of correlation functions $S_{HB}(t)$, $C_{HB}(t)$, and $N_{HB}(t)$ are shown in Figs. 11 and 12, respectively. The results of the corresponding time constants are

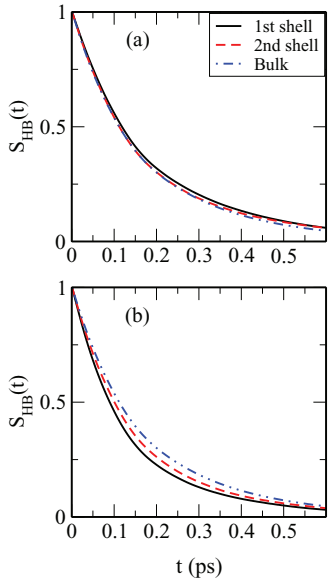

FIG. 11. The plots of continuous hydrogen bond time correlation function $S_{HB}(t)$ in different solvation shells for (a) System 1 and (b) System 2.

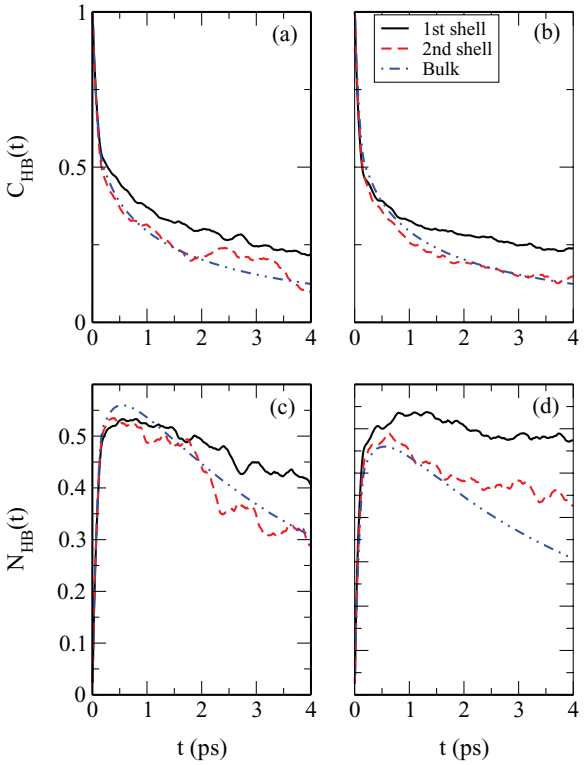

FIG. 12. The decay of the intermittent hydrogen bond correlation functions. (a) and (b) Time dependence of $C_{HB}(t)$ and (c) and (d) show time dependence of $N_{HB}(t)$ functions in different solvation shells of C_{60} and C_{60}^{5-}. The left and right panels are as in Fig. 9.

presented in Table IV. As $C_{HB}(t)$ includes reformation of hydrogen bonds after it breaks along with long time diffusive behavior, its relaxation is much slower than that of $S_{HB}(t)$. Further, a closer look at the relaxation of $C_{HB}(t)$ reveals that $C_{HB}(t)$ for fullerene-ammonia system in different solvation shells decays slightly rapidly than in the corresponding solvation shells in the fulleride-ammonia system. This can be ascribed to the faster rotational and translational motions of solvent molecules in the solvation shells of the neutral C_{60}. Unlike the cases of neutral C_{60} in ammonia system, the continuous hydrogen bond correlation function in the system with charged C_{60}^{5-} decays at a slightly slower rate as the distance between ammonia and C_{60}^{5-} increases (Fig. 11). We note in this context that a similar behavior was also found for water-water

TABLE IV. The values of hydrogen bond relaxation times and average binding energies. τ_{HB} is calculated from the time integral of the continuous correlation $S_{HB}(t)$. τ_{short} and τ_{long} are obtained from the short- (0 − 0.25 ps) and long-time (0.25 − 4 ps) parts of the relaxation of intermittent correlations. The time constants are expressed in ps.

Shell	τ_{HB}	τ_{short}	τ_{long}	E_{av}(kJ/mol)
		System 1		
1	0.20	0.16	0.89	−6.70
2	0.20	0.16	1.18	−6.41
		System 2		
1	0.15	0.12	0.74	−3.21
2	0.17	0.14	0.70	−6.09
Bulk	0.18	0.16	0.68	−6.31

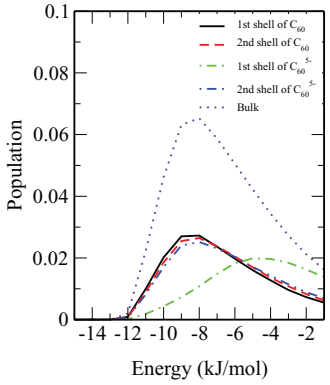

FIG. 13. The binding energy distributions of hydrogen bonded NH_3 pairs in different solvation shells of C_{60} and C_{60}^{5-} for (a) System 1 and (b) System 2.

hydrogen bonds in the vicinity of small ions, e.g., Na^+ where strong electric field was found to induce rapid fluctuations between bonded and non-bonded states of a hydrogen bonded water molecule compared to that in the bulk.[64] In Fig. 13, we have presented the energy distribution of paired hydrogen bonded solvent molecules. For the system with neutral C_{60}, the maxima of distribution in different solvation shells occur approximately at the same energy (E_{max}) corresponding to the bulk value and there is negligible difference in population between them (first shell is slightly higher than second shell). However, a noticeable difference is found for the system with charged C_{60}^{5-}. The maximum of the distribution for the first solvation shell of C_{60}^{5-} is found to occur at a higher energy compared to that for the second solvation shell which has E_{max} value very close to bulk. Also a significant amount of population difference is found to exist among them. The charges of C_{60}^{5-} orient NH_3 molecules in its neighborhood with one hydrogen pointing toward the solute. This oriented arrangement induced by C_{60}^{5-} reduces the ammonia-ammonia interactions as can also be seen from a reduction of the ammonia-ammonia hydrogen bonds discussed in Sec. III.

V. CONCLUSIONS

In the present study, we have investigated the structural and dynamical aspects of ammonia molecules in the vicinity of neutral fullerene and charged fulleride ion. It is found that the ammonia molecules are tightly packed and approach closer toward the fulleride anion in which one of their hydrogen atoms point toward the surface of the negatively charged fullerene. These features do not exist in the solution of the neutral fullerene C_{60} due to solvophobic interaction. Solvation of K^+ mimics the solvation of small positive ions in dipolar liquids. Regarding the dynamics, it is found that the solvent molecules are largely immobilized in the first solvation shell of the charged fulleride ion compared to the case of the neutral fullerene. Consequently, their residence times and orientational relaxation times in the first solvation shell of C_{60}^{5-} are longer than that of the second solvation shell of the fulleride ion. These time scales of the first solvation shell molecules of the fulleride ion are also found to be longer than that of the solvation shells of the neutral fullerene. The

presence of strong electric field is also found to weaken the N−H···N hydrogen bond strength around the fulleride ion leading to a slightly shorter lifetime of ammonia-ammonia hydrogen bonds in the solvation shell of C_{60}^{5-} as compared to that around the neutral fullerene.

ACKNOWLEDGMENTS

We thank the Department of Science and Technology (DST) and Council of Scientific and Industrial Research (CSIR), Government of India, for financial support and also University Grants Commission (UGC) for a research fellowship to M. K. Rana. Part of the calculations was done in the Computer Centre, IIT Kanpur.

[1]C. M. Sayes, J. D. Fortner, W. Guo, D. Lyon, A. M. Boyd, K. D. Ausman, Y. J. Tao, B. Sitharaman, L. J. Wilson, J. B. Hughes, J. L. West, and V. L. Colvin, Nano Lett. **4**, 1881 (2004).
[2]N. Gharbi, M. Pressac, M. Hadchouel, H. Szwarc, S. R. Wilson, and F. Moussa, Nano Lett. **5**, 2578 (2005).
[3]A. Dhawan, J. S. Taurozzi, A. K. Pandey, W. Shan, S. M. Miller, S. A. Hashsham, and V. V. Tarabara, Environ. Sci. Technol. **40**, 7394 (2006).
[4]J. D. Fortner, D. Y. Lyon, C. M. Sayes, A. M. Boyd, J. C. Falkner, E. M. Hotze, L. B. Alemany, Y. J. Tao, W. Guo, K. D. Ausman, V. L. Colvin, and J. B. Hughes, Environ. Sci. Technol. **39**, 4307 (2005).
[5]S. Deguchi, T. Yamazaki, S. Mukai, R. Usami, and K. Horikoshi, Chem. Res. Toxicol. **20**, 854 (2007).
[6]J. Gorman, Sci. News (Washington, D. C.) **162**, 26 (2002).
[7]G. L. Marcorin, T. D. Ros, S. Castellano, G. Stefancich, I. Bonin, S. Miertus, and M. Prato, Org. Lett. **2**, 3955 (2000).
[8]D. W. Cagle, S. J. Kennel, S. Mirzadeh, J. M. Alford, and L. J. Wilson, Proc. Natl. Acad. Sci. U.S.A. **96**, 5182 (1999).
[9]T. Wharton, J. M. Alford, L. O. Husebo, and L. J. Wilson, *Paramagnetic Malonodiamide Derivatives of C_{60} as MRI Contrast Agent Precursors* (Electrochemical Society, Pennington, NJ, 2000), Vol. 9, p. 258.
[10]N. Tsao, T.-Y. Luh, C.-K. Chou, T.-Y. Chang, J.-J. Wu, C.-C. Liu, and H.-Y. Lei, J. Antimicrob. Chemother. **49**, 641 (2002).
[11]H. T. Tien and A. L. Ottova, Electrochim. Acta **43**, 3587 (1998).
[12]I. Szymanska, H. Radecka, J. Radecki, and D. Kikut-Ligaj, Biosens. Bioelectron. **16**, 911 (2001).
[13]C. Toniolo, A. Bianco, M. Maggini, G. Scorrano, M. Prato, M. Marastoni, R. Tomatis, S. Spisani, G. Palu, and E. D. Blair, J. Med. Chem. **37**, 4558 (1994).
[14]S. Deguchi, R. G. Alargova, and K. Tsujii, Langmuir **17**, 6013 (2001).
[15]R. G. Alargova, S. Deguchi, and K. Tsujii, J. Am. Chem. Soc. **123**, 10460 (2001).
[16]W. A. Scrivens and J. M. Tour, J. Am. Chem. Soc. **116**, 4517 (1994).
[17]G. V. Andrievsky, V. K. Klochkov, E. L. Karyakina, and N. O. Mchedlov-Petrossyan, Chem. Phys. Lett. **300**, 392 (1999).
[18]G. V. Andrievsky, V. K. Klochkov, A. B. Bordyuh, and G. I. Dovbeshko, Chem. Phys. Lett. **364**, 8 (2002).
[19]P. Scharff, K. Risch, L. Carta-Abelmann, I. M. Dmytruk, M. M. Bilyi, O. A. Golub, A. V. Khavryuchenko, E. V. Buzaneva, V. L. Aksenov, M. V. Avdeev, Y. I. Prylutskyy, and S. S. Durov, Carbon **42**, 1203 (2004).
[20]J. F. Maguire, M. S. Amer, and J. Busbee, Appl. Phys. Lett. **82**, 2592 (2003).
[21]M. S. Amer, J. A. Elliott, J. F. Maguire, and A. H. Windle, Chem. Phys. Lett. **411**, 395 (2005).
[22]R. Rivelino, A. M. Maniero, F. V. Prudente, and L. S. Costa, Carbon **44**, 2925 (2006).
[23]T. Malaspina, E. E. Fileti, and R. Rivelino, J. Phys. Chem. B **111**, 11935 (2007).
[24]J. C. Rasaiah, S. Garde, and G. Hummer, Annu. Rev. Phys. Chem. **59**, 713 (2008).
[25]G. Hummer, J. C. Rasaiah, and J. P. Noworyta, Nature (London) **414**, 188 (2001).
[26]N. Choudhury and B. M. Pettitt, J. Am. Chem. Soc. **127**, 3556 (2005).
[27]N. Choudhury and B. M. Pettitt, J. Phys. Chem. B **110**, 8459 (2006).
[28]M. C. Gordilo and J. Marti, J. Phys.: Condens. Matter **22**, 284111 (2010).
[29]J. Marti, J. Sala, and E. Guardia, J. Mol. Liq. **153**, 72 (2010).
[30]M. V. Athawale, S. N. Jamadagni, and S. Garde, J. Chem. Phys. **131**, 115102 (2009).
[31]B. Mukherjee, P. K. Maiti, C. Dasgupta, and A. K. Sood, J. Phys. Chem. B **113**, 10322 (2009).
[32]S. Joseph and N. R. Aluru, Nano Lett. **8**, 452 (2008).
[33]L. Li, D. Bedrov, and G. D. Smith, Phys. Rev. E **71**, 011502 (2005).
[34]L. Li, D. Bedrov, and G. D. Smith, J. Chem. Phys. **123**, 204504 (2005).
[35]L. Li, D. Bedrov, and G. D. Smith, J. Phys. Chem. B **110**, 10509 (2006).
[36]N. Choudhury, J. Chem. Phys. **125**, 034502 (2006).
[37]N. Choudhury, J. Phys. Chem. B **111**, 10474 (2007).
[38]N. Choudhury, J. Phys. Chem. C **111**, 2565 (2007).
[39]R. S. Ruoff, D. S. Tse, R. Malhotra, and D. C. Lorents, J. Phys. Chem. **97**, 3379 (1993).
[40]C. A. Howard, H. Thompson, J. C. Wasse, and N. T. Skipper, J. Am. Chem. Soc. **126**, 13228 (2004).
[41]C. A. Howard, J. C. Wasse, N. T. Skipper, H. Thompson, and A. K. Soper, J. Phys. Chem. C **111**, 5640 (2007).
[42]C. A. Howard and N. T. Skipper, J. Phys. Chem. B **113**, 3324 (2009).
[43]S. Koneshan, J. C. Rasaiah, R. M. Lynden-Bell, and S. H. Lee, J. Phys. Chem. B **102**, 4193 (1998).
[44]A. Chandra and S. Chowdhuri, J. Phys. chem. B **106**, 6779 (2002).
[45]J. Gao, X. Xia, and T. F. George, J. Phys. Chem. **97**, 9241 (1993).
[46]L. A. Girifalco, J. Phys. Chem. **96**, 858 (1992).
[47]U. Essmann, L. Perera, M. L. Berkowitz, T. Darden, H. Lee, and L. G. Pedersen, J. Chem. Phys. **103**, 8577 (1995).
[48]M. P. Allen and D. J. Tildesley, *Computer Simulation of Liquids* (Oxford University Press, New York, 1987).
[49]S. Margadonna, E. Aslanis, and K. Prassides, J. Am. Chem. Soc. **124**, 10146 (2002).
[50]N. Choudhury, J. Chem. Phys. **133**, 154515 (2010).
[51]J. C. Wasse, S. Hayama, N. T. Skipper, C. J. Benmore, and A. K. Soper, J. Chem. Phys. **112**, 7147 (2000).
[52]A. Tongraar, S. Hannongbua, and B. M. Rode, Chem. Phys. **219**, 279 (1997).
[53]A. H. Narten, J. Chem. Phys. **66**, 3117 (1977).
[54]H. Thompson, J. C. Wasse, N. T. Skipper, S. Hayama, D. T. Bowron, and A. K. Soper, J. Am. Chem. Soc. **125**, 2572 (2003).
[55]S. Paul and A. Chandra, J. Chem. Phys. **123**, 174712 (2005).
[56]S. Chowdhuri, and A. Chandra, J. Phys. Chem. B **110**, 9674 (2006); B. S. Mallik and A. Chandra, J. Chem. Phys. **125**, 234502 (2006).
[57]D. C. Rapaport, Mol. Phys. **50**, 1151 (1983).
[58]G. Sutmann and R. Vallauri, J. Phys.: Condens. Matter **10**, 9231 (1998).
[59]A. Luzar, J. Chem. Phys. **113**, 10663 (2000).
[60]A. Chandra, Phys. Rev. Lett. **85**, 768 (2000); J. Phys. Chem. B **107**, 3899 (2003).
[61]S. Balasubramanian, S. Pal, and B. Bagchi, Phys. Rev. Lett. **89**, 115505 (2002).
[62]A. Luzar and D. Chandler, Phys. Rev. Lett. **76**, 928 (1996); Nature (London) **379**, 55 (1996).
[63]H. Xu and B. J. Berne, J. Phys. Chem. B **105**, 11929 (2001).
[64]H. Xu, H. A. Stern, and B. J. Berne, J. Phys. Chem. B **106**, 2054 (2002).